INTERSTELLAR ABSORPTION LINES IN DISTANT STARS

I. NORTHERN MILKY WAY

Guido Münch
Mount Wilson and Palomar Observatories
Carnegie Institution of Washington, California Institute of Technology
Received July 16, 1956; revised September 14, 1956

ABSTRACT

Measures of radial velocities and intensities of the Ca II and/or Na I interstellar lines are given for 112 stars near the galactic plane and with longitudes between 55° and 160°. In stars at distances not smaller than about 2 kpc two strong components are observed, with relative separations depending on galactic longitude and reaching a maximum of about 30 km/sec around $l = 100°$. It is shown that this separation is an effect of galactic rotation, and it is inferred that the interstellar gas clouds producing the observed lines are arranged in space along the spiral arms outlined by the space distribution of H II regions. The connection between data derived from the optical absorption lines and other indicators of spiral structure, such as the space distributions of O associations and interstellar hydrogen, is discussed. It is found that the interstellar gas around distant O associations has systematic expanding motions, revealed by line components shifted to the violet with respect to the velocities of the associations by amounts of the order of 20 km/sec.

The mean intensity-ratio-curves of the Na I and Ca II doublets in nearby stars are rediscussed. It is shown that they may be accounted for by a velocity distribution of the interstellar clouds exponential in form and with mean speed η constant within a spiral arm rather than by a Gaussian distribution with dispersion increasing with distance from the observer. An indication has been found that the η(Na I) for the lines formed in the Perseus arm is larger by factors between 1.2 and 1.5 than for the lines formed in the Orion arm. The existence of variations in shape of the velocity distribution of the interstellar clouds, in relation to the geometry of the spiral arms, is suggested.

I. INTRODUCTION

Observations of interstellar absorption lines in stars of the northern Milky Way have been made so far only with relatively low spectroscopic resolving power. The mechanical features in the mounting of the 100-inch telescope at Mount Wilson prevented W. S. Adams (1949) from extending his observations with the coudé spectrograph to stars north of $\delta = +50°$. If the regions of Perseus and Cepheus, where distant early-type supergiants appear relatively bright, had been accessible to the 100-inch coudé, no doubt the structural features of the galactic system, now recognized as its spiral arms, would have been discovered at least a decade earlier. And it was not until the coudé spectrograph of the 200-inch reflector was put into operation that high-dispersion spectra of stars near $l = 100°$ were obtained. As was announced in an earlier note (Münch 1953), the structure of the interstellar absorption lines in these stars immediately verified the concentration of the interstellar gas along the features first outlined by Morgan, Osterbrock, and Sharpless (1952) as the spiral arms of the galactic system. Since this preliminary discussion appeared, sufficient data have been collected on a number of additional stars to make appropriate the publication of a detailed study of the intensities and radial velocities of their interstellar absorption lines. A comparison of the results of our study with those derived from the analysis of the early Mount Wilson observations (Merrill, Sanford, Wilson, and Burwell 1937; Sanford and Wilson 1939) and with the data recently obtained from the observation of the emission line of hydrogen at 21 cm wave length (van de Hulst, Müller, and Oort 1954) is also contained in this paper.

II. OBSERVATIONAL DATA

In the summer of 1951 Dr. W. W. Morgan kindly put at my disposal his then unpublished list of spectroscopic distance moduli for early-type stars. An inspection of this list revealed that a large number of distant stars, not included in Adams' survey, could still be observed in coudé dispersions. The desirability of enlarging our information in regard to the behavior of the interstellar lines at large distances from the sun is apparent when it is considered that no more than 10 per cent of the 300 stars observed by Adams have distances larger than 1 kpc and only 2 of them are found at a distance greater than 2.5 kpc. It was decided, accordingly, to start observing, with the coudé spectrograph of the 100-inch reflector, the strong interstellar lines (H and K of Ca II and/or the D lines of Na I) in the spectra of nearly 200 stars. Most of these objects are too faint for the camera of longest focal length (114-inch) but still within reach of the 72- or 32-inch Schmidt cameras. With the fastest camera it is possible to obtain, in a II*a*-O emulsion baked for 72 hours at 50° C, the blue spectrum (10 A/mm dispersion) of a star of $m_{pg} = 10$, widened to 0.1 mm, with an exposure time of 5 hours in good seeing conditions.

When the Palomar coudé became available one year later, the program was extended to stars with $\delta > +50°$, giving special consideration to the problem of detecting, in the interstellar gas, a large-scale arrangement in space, of the kind shown by the distribution of H II regions (Morgan *et al.* 1952). From the start of the observations at Palomar it was realized that only a few of the distant stars could be reached with the 12-foot camera and that the cameras with half and one-quarter that focal length would be more suitable for our purpose. The 72-inch camera (Bowen 1952) and the mosaic grating available give dispersions of 4.5 A/mm in the third-order blue and 6.8 A/mm in the second-order yellow. The resolving power of spectra taken with it is, in practice, determined by the slit width used, which in our case was set to correspond in projection to the resolving power of the emulsions used: 20 μ for the II*a*-O plates and 25 μ for the 103*a*-D emulsion. The same consideration applies to the 36-inch camera. Because the H and K lines in the third-order spectrum fall very near the position of the D lines in the second order, it was not possible to photograph the two sets of lines simultaneously.

Data relevant to the stars observed are given in Table 1. The first two columns identify the stars by their catalogue numbers and galactic co-ordinates (l, b) referred to the Lund pole. In the third column appear the spectral types and distance moduli, $m_0 - M$, derived from the data given by Morgan, Code, and Whitford (1955). The number of the association to which the star may belong, according to Morgan, Whitford, and Code (1953), is given in the fourth column. In the fifth column are given, on top, the heliocentric radial velocities of the stars and, below, the corrections for local solar motion. Most of the radial velocities and their weights have been adopted from the Mount Wilson *Catalogue* (Wilson 1953). For a few stars of special interest not contained in this catalogue, the radial velocities have been measured, when at all feasible, on the same coudé plates as those taken for the interstellar lines, otherwise in special low-dispersion plates taken with the new Cassegrain grating spectrograph of the 60-inch Mount Wilson telescope. These measured velocities are distinguished in the table by the letter "m" which follows their values. The solar motion used for computing the reduction to the local standard of rest is the one determined by Blaauw (1952), $V_0 = 20$ km/sec toward $l = 19.°1$ and $b = +22.°8$. The sixth column indicates the lines observed and the instrument used in the observation. The letters "O" and "D" denote whether the Ca II or the Na I lines are concerned. The symbols "P" and "C" are used to distinguish between plates taken at Palomar and those taken at Mount Wilson, while the letters "a," "b," and "c" indicate the camera or cameras used, in order of their focal distance and starting with the longest one. For example, a symbol OPbbc means that the Ca II lines were observed at Palomar on two plates taken with the 72-inch camera and also on one 36-inch plate. In the seventh column the quality assigned to the particular observation is indicated by one of the letters "A," "B," "C," and "D," which was assigned according to the cameras used and the widths, densities, and graininess of the spectra available. To a spectrum taken with the 72-inch camera, exposed to optimum density and widened

TABLE 1

RADIAL VELOCITIES AND INTENSITIES OF INTERSTELLAR LINES IN DISTANT STARS
($55° < l < 160°$)

STAR HD	l° b°	SPECTRUM mo − M	Assoc.	V ΔV (km/sec)	PLATES		Quality	RADIAL VELOCITIES km/sec			INTENSITIES (m A) K or D2		H or D1	
202124*	55.1	O9.5 Ib		−43m	O	Pb	A	−56	−40	− 8	46 (3) 89 (7)	398	28 (4) 43 (7)	22
	−3.2	12.6		+15.3	O	Cc			−47	− 6				
199216	56.6	BI II		− 6.6b	O	Cb	B		−20	−13	I	214		14
	−2.3	10.1		+14.9	O	Cc				−14				
203938	58.3	B0.5 IV		−	O	Cc	D			−12		270		15
	−2.7	8.8		+13.9										
208220	60.0	BI IVe		−39e	O	Pc	C		−43	−15	164 (1)	312	111 (1)	20
	−8.9	13.6:		+12.6										
204827	66.7	BOV	15	−	O	Pc	C			−18		268		19
	+5.3	9.7		+13.1										
206773	67.4	B0 Vp	15	−22c	O	Pc	D			−14		320		20
	+3.4	9.6		+12.7										
209900*	67.4	A0 IB	16	−63m	D	Pc	C	−60	−37	−10	144 (1) 222(1)	687	109 (1) 165 (2)	60
	−2.0	−		+12.0										
210809	67.7	O9 Ib	16	−80c	O	Pb	B		−41	−11	185 (3)	290	113 (5)	19
	−3.4	12.4		+11.7	O	Pc			−46	−14				
205139	68.1	BI II	15	−14.5	O	Pa	B	−28	−18	− 8	36 (1) 171 (1)	46	23 (1) 112 (1)	3
	+6.4	9.7		+ 8.4										
209481 14 Cep	69.	O9V	15	−11c	O	Pa	B		−22	−10	I	259		16
	+2.0	8.9		+12.0										
206165	69.8	B2 Ib	15	−22.2b	O	Pa	Bs		−36	−18	I	179		12
	+7.0	9.1		+12.6										
212455	70.6	B5Iab	16	−59c	D	Pb	B		−46	−16	641 (1)	604	517 (3)	56
	−2.1	12.7		+11.2										
207198	70.7	O9 II	15	−18.4b	O	Pa	B			−16		260		18
	+6.9	9.9		+12.3										
210839	71.5	O6f		−74c	O	Pa	B		−34	−11	I	214		17
	+2.5			+11.6										
209975 19 Cep	72.4	O9.5 Ib		−12.8a	O	Pa	B			−14		191		16
	+5.3	10.3		+11.7										
213470*	72.4	A3Ia	16	−60.8b	O	Pb	B	(−55	−39)	−15	528 (6)	499	418 (7)	42
	−0.7	12.5:		+11.0										
214419	72.4	O7+WR	16	−75b	O	Pc	D		−34	−10	151 (2)	405	101 (4)	35
	−1.4			+10.6										
216438*	73.6	BI II		−85m	O	Pcc	B		−63	−16	222 (6)	311	102 (5)	22
	−5.2	13.0		+10.0										
215835	74.8	O6	16	−	O	Pc	D		−41	−19	93 (2)	364	60 (3)	25
	−1.3			+10.1										
216411	75.7	BI Ia		−44c	O	Pb	A	(−61	−49)	−15	126 (7)	467	86 (7)	33
	−0.4	11.8		+10.2	O	Pc			−60	−17	137 (2)	393	75 (2)	28
					D	Pb	B	(−62	−47)	−14	278 (3)	519	155 (4)	45
218915*	76.0	O9 I												
	−6.9	12.6		−72.ob	O	Pa	A	(−52	−27)	−13	140 (8)	248	76 (9)	16
				+9.1	O	Pb		(−55	−30)	−14	153 (6)	235	86 (9)	14
					O	Pc		−58		−15	134 (4)	205		
					O	Xd		−48		−13				
213087	76.1	B0.5 Ib		−14.7b	O	Pa	B		−24	−17	I	235		18
	+6.3	10.1		+10.8										
216927	76.2	B9 Ia	16	−42m	D	Pc	C		−54	−17	444 (1)	600	351 (1)	53
	−0.3	13.3		+10.0										
216532	77.3	O8	17	−	O	Pc	C			−16		317		23
	+2.6			+10.1										
218376 1 Cas	77.7	B0.5 IV		− 8.5b	O	Pa	B			−12		220		12
	−0.8	8.5		+9.6										
223385* 6 Cas	83.4	A3 Ia+	18	−45.6a	D	Pbb	A	(−61	−50)	−16	363 (5)	740	231 (5)	60
	+0.4			+8.1	D	Pc								
223960*	83.7	AOIa		−48.1b	D	Pbb	B	(−59	−42)	(−23 −8)	503 (1)	515	494 (2)	50
	−1.1	11.9		+7.8										
223987	83.9	B1.5 Iab	18	−44.8b	O	Pc	D		−57	− 6	317 (2)	334	145 (3)	18
	−0.4	12.0		+7.9										
224055*	84.0	B3Ia	18	−43.3b	O	Pb	Bs		−59	(−17 −5)	251 (3)	315	214 (4)	29
	−0.1	11.6		+7.9										
224424	84.0	BI Iab		−71c	O	Pc	D		−50	−15	98 (1)	330	def (1)	25
	−2.3	12.2		+7.6										
225146	85.0	BOIbp		−29.0b	O	Pc	D	(−61	−41)	−12	277 (2)	411	190 (2)	24
	−1.1	13.2		+7.3	D	Pc	C		−51	−11	94 (4)	564	94 (4)	52
225160	85.1	O8f		−46d	O	Pcc	C	(−60	−42)	−11	187 (1)	371	136 (2)	27
	+0.1			+7.5										
225094*	85.3	B3Ia		−43c	O	Pab	As	(−65	−38)	− 8	278 (5)	358	202 (5)	30
	+1.4	11.8		+7.7	D	Pab	A				92 (4)	640	59 (5)	58

	STAR HD	l° b°	SPECTRUM mo-M	Assoc.	V (km/sec) ΔV	PLATES		Quality	RADIAL VELOCITIES km/Sec			INTENSITIES (m A) K or D2		H or D1	
2	108*	85.6	O8fp		-62.8b	O	Pbc	B	(-68	-42)	- 7	130 (7)	381	126 (8)	30
		+1.4			+7.6										
6	1337*	85.6	O9 III		-35.2b	O	Pb	A	(-42	-31)	(-17 -10)	125 (2)	180	080 (3)	13
	AO Cas	-10.9	11.8		+5.9	O	Ca								
0	1383	86.7	BI II	19	-40c	O	Pc	C		-43	-12	254 (3)	378	164 (4)	26
		-0.7	11.6		+7.0										
9	1544	87.0	B0 III	19	-41b	O	Pc	C		-40	-13	107 (3)	286	61 (4)	18
		-0.3	11.8		+6.9										
2	1743	87.2	B0 III	19	-32d	O	Pc	D		-62	-18	74 (5)	334	50 (5)	26
		-0.2	11.8		+6.9										
1	1810	87.3	B0 IV	19	-47c	O	Pc	D		-67	-14	53 (8)	314	32 (8)	19
		-0.2	11.3		+6.9										
7	2451	88.0	B0.5 IV	19	-48d	O	Pc	D		-68	-21	II	368		23
		0.0	12.1		+6.9										
0	2905	88.5	BI Ia		-2.3a	O	Pa	Bs		-23	-16	I	246		16
	κ Cas	+0.5	10.2		+6.6										
5	3940*	89.7	AI Ia	20	-48m	D	Pc	C		-60	-16	105 (6)	690	53 (6)	58
		+1.7	12.4		+6.5										
9	4717	90.5	AO Ib	20	-50d	D	Pc	C		-56	-15	120 (5)	561	75 (6)	50
		+0.6	11.9		+6.1										
5	4768	90.6	B5 Ib	20	-39c	D	Pc	C		-44	-18	I	725		53
		-2.9	12.1		+5.5										
3	4841	90.6	B5 Ia	20	-26c	D	Pbb	A	(-60	-37)	-11	108 (8)	808	66 (9)	73
		+1.2	12.1		+6.1										
4	5551*	91.4	B1.5 Ib	20	-51c	O	Pbc	Bs	(-66	-41)	-15	232 (3)	302	145 (4)	21
		+1.2	11.4		+5.8										
0	6182	92.0	BI Ibp		-43c	O	Pc	D		-45	-16	88 (7)	495	48 (8)	44
		-0.1	12.5		+5.4										
0	6675*	92.0	B0.5 III		-	D	Pb	C		(-12	+12)		277		21
		+7.3	10.4		+6.4										
5	7103	93.1	B3 Ib		-	O	Pc	Cs	(-65	-42)	-18	240 (3)	398	156 (4)	28
		-0.5	11.9		+5.0										
2	7902	94.5	B6 Ib		-31d	D	Pb	B		-49	-15	382 (2)	601	249 (3)	55
		-4.0	12.5		+4.2										
0	9105	95.1	B5 Iab		-37.3b	D	Pb	B		-61	-13	208 (2)	1040	139 (3)	90
		+1.3	11.8		+4.7										
0	9311*	96.0	B5 Ib		-38.9d	D	Pb	B	(-65	-50)	-14	129 (2)	622	77 (3)	59
		-1.3	11.4		+4.3										
0	10125	96.0	O9.5 Ib		-	O	Pc	C		-56	-16	90 (2)	398	50 (3)	24
		+2.3	13.0:		+4.5										
4	12301	98.2	B8 Ib		-20.0b	D	Pbb	A			- 6		421		37
		+3.1	9.9		+4.9										
0	14010	99.8	B9 Ia		-48.4b	D	Pbb	A		-52	-10	256 (6)	625	153 (8)	58
		+3.8	12.6		+4.4										
5	12953	100.7	AI Ia	21	-36.3a	D	Pbb	A	(-60	-44)	-11	350 (6)	650	230 (7)	60
		-2.4	11.9		+2.4										
0	13402	100.9	B0.5 Ip		-	O	Pc	C		-54	-12	96 (7)	258	81 (8)	24
		-1.1	12.5:		+2.5										
0	13267	101.3	B5 Ia	21	-33.8b	D	Pb	C		-58	-10	390 (5)	550	260 (4)	49
		-3.0	12.3		+2.1										
3	13476	101.3	A3 Iab	21	-40.5b	D	Pb	B	(-60	-38)	-10	449 (3)	590	358 (4)	57
		-2.0	11.5		+2.2										
9	13841	102.2	B2 Ib	21	-39.0b	O	Pbb	As	(-59	-41)	- 8	359 (3)	315	180 (3)	24
		-3.3	12.0		+1.8										
7	13854	102.2	BI Iab	21	-40.2b	O	Pab	As	(-51	-31)	-10	356 (5)	303	186 (6)	21
0		-3.3	11.7		+1.8	D	Pb	B	-55	-43	-11	354 (7)	570	293 (7)	51
3	13866	102.3	B2 Ib	21	-47.0b	O	Pc	Cs		-46	- 9	194 (2)	364	116 (3)	31
		-4.3	12.1		+1.7										
0	13745	102.4	BO III	21	-29.5b	O	Pc	C		-56	-11	207 (4)	245	120 (4)	18
		-4.3	11.4		+1.6										
2	14134*	102.4	B3 Ia	21	-43.7b	O	Pbb	As	(-68	-52)	-10	362 (3)	272	203 (4)	16
4		-3.1	12.2		+1.7	D	Pbb	A	(-66	-53)	-14	351 (6)	680	264 (7)	57
2	14143*	102.4	B2 Ia	21	-41.7b	O	Pab	As	(-64	-49)	- 6	420 (3)	300	240 (4)	19
5		-3.1	11.9		+1.7	D	Pbb	A	(-64	-48)	-10	531 (4)	690	406 (5)	58
3	15558	102.4	06		-50c	O	Pc	C	(-52	-31)	-11	73 (4)	366	39 (5)	27
		+1.6			+2.4										
5	14433	102.7	AI Ia	21	-46.7b	D	Pb	B		-50	-12	250 (5)	659	148 (6)	56
		-2.9	12.2		+1.6										
3	14542	102.8	B8 Ia	21	-47.4b	D	Pbb	A	(-59	-40)	- 9	285 (5)	714	186 (6)	64
		-2.7	12.0		+1.7										

1957ApJ...125...42M

STAR HD	l° b°	SPECTRUM mo − M	Assoc.	V ΔV (km/sec)	PLATES		Quality	RADIAL VELOCITIES km/sec			INTENSITIES (m A) K or D2		H or D 1	
15785	103.0	BI lab		-	O	Pc	D		-56	-13	72 (3)	350	def	2
	+0.8	13.0		+2.0										
14322	103.1	B8 Ib	21	-35c	D	Pb	C		-44	-12	277 (3)	594	161 (4)	4
	-4.2	11.4		+1.3										
14956	103.2	B2 Ia	21	-24c	O	Pb	Cs		-54	- 9	190 (4)	298	110 (4)	2
	-2.2	12.0		+1.6										
14489*	103.3	A2 Ia	21	-15.2a	D	Pb	C		-39	-10	I	696		6
	-4.2	11.5		+1.2										
14818*	103.4	B2 Ia	21	-46.0b	O	Pabb	As	(-44	-35)	- 8	320 (5)	278	171 (6)	2
	-3.3	11.5		+1.4	D	Pbb	A	(-50	-35)	- 9	369 (3)	480	243 (4)	4
17857	103.5	B8 Ib		-	D	Pc	C		-61	-14	380 (4)	422	318 (5)	3
	+5.1	11.4		+2.4										
15497	103.8	B6 Ia	21	-39c	D	Pb	B		-50	-17	383 (2)	626	337 (3)	5
	-1.9	11.6		+1.5										
17505	104.9	O7		-17c	O	Pbb	B		-44	- 8	236 (1)	290	151 (2)	1
	+1.6			+1.6										
17088	105.6	B9 Ia		-42.3b	D	Pb	B		-55	- 9	524 (7)	622	488 (8)	61
	-1.0	12.2		+1.0										
17145	105.7	B8 Ia		-	D	Pc	C		-47	-13	331 (2)	707	243 (3)	5
	-1.1	12.4		+0.9										
14633	108.9	O8		-36c	O	Cb	B		-34	- 6	92 (2)	270	50 (2)	2
	-17.4	11.8		+2.3		Cc						320		22
21291	109.1	B9 Ia	22	-6.8b	D	Pbb	A		-35	- 8	I	552		5
	+3.7	10.2		+0.5										
25638	111.2	BO II-III		- 9d	O	Pa	B		(-10	+ 2)		224		1
	+8.5	9.9		+0.5										
30614	111.4	O9.5 Ia		+6.1a	O	Pbb	A		(-13	+ 1)	I	282		2
α Cam	+14.9	10.7		+1.3										
22253	112.0	B0.5 III	22	+5c	O	Pc	C			- 5		224		15
	+1.7	9.9		-1.8										
+55°837*	114.6	B2 Ib		-81m	O	Pc	C		-37	- 1	240 (3)	346	205 (4)	30
	+2.9			-1.4										
237213*	115.2	B3 Ia			O	Pc	Cs		-41	- 1	248 (3)	366	162 (4)	34
	+3.6			-1.2										
25914	115.4	B6 Ia		-26e	D	Pcc	C		-45	-13	660 (2)	614	585 (3)	53
	+4.8	13.2		-1.4										
24432	116.5	B3 II	22	-10.8b	O	Cbc	B			-7		329		24
	0.0	9.7		-2.1				-26	(-10	- 1)	I	330		27
232947*	119.2	BOIa		-48e	O	Pc	C		-38	- 3	240 (3)	340	135 (4)	25
	+3.9			-2.7										
28446	119.5	BO III		-7c	O	Pb	B			- 1		208		14
	+4.9	9.3		-2.7										
25517	123.3	B1 V		-	O	Ccc	C		-27	- 6	I	443		29
	-4.9	11.1		-5.2										
232999*	123.3	BI IV		-27m	O	Cc	C		-22	- 1	165 (3)	197	102 (4)	15
	+4.2			-4.0										
+43°1168	130.5	B9 lab		-22m	D	Cc	D		-18:	0:	430(1)	480	340 (2)	44
	+2.4			-6.4										
31327	135.9	B2 III		-5c	O	Ccc	As		+4			296		19
	-3.1	7.5		-8.7	O	Cb			- 6	+ 8	92 (2)	210	40 (2)	14
34656	137.7	O7	24	-	O	Cb	B		(-6	+11)		298		18
	+1.6			-8.6										
34921	137.7	B0 IVpe	24	-9.c	O	Cc	C			+ 6		211		13
	+2.0	10.1		-8.3										
34078	139.8	O9.5 v		+59.1a	O	Cc	C			+15		135		9
AE Aur	-0.9	8.8												
35921	140.4	O9.5 III	24	-29d	O	Ccc	B		(-10	+ 5)		267		21
	+1.9	10.3		-9.4										
35619*	140.7	O8		-	O	Cc	C		-23	+ 4	I	317		18
	+1.7			-9.4										
35633	140.9	B0.5 IV	24	-	O	Cc	C			+ 5		201		17
	+1.1	10.4		-9.5										
242908*	141.2	O5		-	O	Cc	C			+ 3		390		26
	-0.3			-9.8										
242926*	141.2	O6		-8d	O	Cc	C			- 2		360		30
	-0.4			-9.8										
242935*	141.2	O7		-	O	Cc	c			+ 1		347		26
	-0.4			-9.8										

STAR HD	l° b°	SPECTRUM mo–M	Assoc.	V ΔV (km/sec)	PLATES		Quality	RADIAL VELOCITIES km/sec		INTENSITIES (m A) K or D2	H or D1
35653	141.4 +0.8	B0.5 V 9.8		+3c −9.7	O	Cc	C		+9	318	21C
39746	149.9 +2.7	BI II 11.1	25	−11.7	O	Cc	C		+14	264	216
41398	149.9 +5.3	B2 Ib 11.9	25	+17.9 b −11.4	O	Cc	Cs	−5	+ 7	475	306
36879*	153.3 −4.5	O6	25	−13.5	O	Cc	C		+13	304	223
43384 9 Gem	155.7 +5.0	B3 Iab 11.3	25	+13.2b −12.6	D	Cb	B	(+6	+19)	566	47C
43818	156.2 +5.3	BO II 10.7	25	+18.2b −12.7	O	Cc	C		+17	321	19C
43753	156.6 +5.0	B0.5 III 11.2	25	−12.8	O	Cc	C		+10	430	305
43078	156.8 +4.0	B0.5 III 11.4	25	−13.1	O	Cc	C		+11	423	26C
42379	157.0 +2.8	BI II 11.3	25	−13.3	O	Cc	C		+13	292	21C
42088	157.7 +1.9	O6	25	+23.4b −13.6	O	Cc	C		+16	336	228

NOTES TO TABLE 1

HD 202124 Component at +14 km/sec I W (K) = 80 m A. V = −40 ± 2 km/sec from 2 Xf plates.
HD 209900 V = −63.2 ± 1.0 km/sec from 11 lines in Pc plate.
HD 213470-1 V = −64.2 ∓ 0.6 km/sec from 9 lines in Pb plate.
HD 216438 V = −84.7 ∓ 1.4 km/sec from 2 Pc plates.
HD 218915 Xd plate, dispersion 20.6 A/mm, shows clearly double character of interstellar K line.
HD 223385 Components at +7.8 and 21.4 km/sec. Combined intensities W (D2) = 98 m A, W (D 1) = 69 m A.
HD 223960 Component at +8 km/sec.
HD 224055 Possible component of K at −87 km/sec.
HD 225146 V = −53 + 4 km/sec from 8 lines in D Pc plate, discordant with published value. V variable?
HD 225094 Components of K at −94, −79, −18, +9 and +26 km/sec.
HD 108 Component at −20 km/sec.
HD 1337 Component at −17 km/sec.
HD 3940 V = −4.9 ± 2 from 11 lines in D Pc plate.
HD 5551 Possible components at +14 and +33 km/sec.
HD 6675 Component at +12 km/sec.
HD 9311 Component at +25 km/sec.
HD 14134 Possible component at −38 km/sec.
HD 14143 Possible component at −33 km/sec.
HD 14489 V = −20.6 ± 1.8 from 20 lines in K Pb plate. Trace of component at −39 km/sec. Probably star does not belong to the association I Per and it is at a smaller distance than spectroscopic parallax indicates.
HD 14818 Possible component at −61 km/sec.
BD +55°837 V = −81 ± 4 km/sec from 10 lines in 1 Xf plate.
HDE237213 V = +14 km/sec published previously disregarded because of low weight.
HDE232947 V = −49 ± 6 km/sec from 6 lines in 1 Xf plate.
HDE232999 V = −27 ∓ 1 km/sec from 2 Xf plates. V = +1 km/sec published previously disregarded because of low weight.
HD 35619 Possible K component at −67 km/sec.
HDE 242908, 242946 and 242935. Stars in cluster IC 410.
HD 36879 Possible K component at +59 km/sec.

to 0.3 mm, a quality B is assigned. A similar spectrum taken with the 36-inch camera has quality C. The symbol "A" is attached to observations based on more than one good plate, and quality "D" results from plates not properly exposed or not widened enough to consider them photometrically reliable. A letter "s" following the quality symbol indicates that the presence of stellar Ca II lines was noticed in the microphotometer tracings. Succeeding columns in Table 1 contain data related to the radial velocities and line intensities measured, which are described in detail in the next two sections.

III. MEASUREMENTS

a) Radial Velocities

The structure of the interstellar lines in many of the stars in Table 1 is very complex (Figs. 1 and 2). The strong features often give indication of being formed by the superposition of a number of lines, not quite fully resolved because of insufficient resolving power and Doppler shifts. The measurement, with a conventional micrometer, of the wave lengths of the apparent maxima or minima in such complex lines does not lead to radial velocities accurate to the degree set by the internal consistency of the settings. To assign a "probable error," as is usually done, from the standard deviation of a set of measures has little meaning. If instrumental broadening predominates, it is clear that the radial velocities of partially overlapping absorption features will not be the same in spectra of different dispersions. And even plates of identical dispersion but different levels of exposure may lead to different results. By determining the line profiles, of course, the effects of instrumental broadening could be accounted for; but the observational material required to make the photometry accurate enough would have to be much more extensive than ours is. Since it is believed that our observations do not justify a more elaborate procedure, the radial velocities of the various components of the interstellar lines have been measured in the conventional fashion. The cross-wire of the micrometer was set in the middle of every feature appearing to the eye as an absorption line. The corresponding radial velocities were assumed to be the straight means of the values derived for both members of the doublet. It is realized that this averaging procedure is not strictly correct, for the intensity ratio of the doublet is not constant for all the components of a blend and consequently the velocities of the same blend in the two members of the doublet are not necessarily identical. While in one extreme case we have noticed a difference of 3 km/sec on this account, probably on the average it will be less than 1 km/sec and may be safely neglected.

The majority of the complex lines listed in Table 1 consist of a very strong component with a small displacement to the violet and another main feature shifted farther to the violet by amounts varying between 30 and 50 km/sec. For brevity, we shall refer in the future to these two features as the R- and V-components, respectively. In many cases the V-component itself shows two or even more subcomponents, which we shall refer to as the V1, V2, . . . , components, in the order of increasing velocities. In the eighth column of Table 1 we list the heliocentric radial velocities of the R- and V-features, or of the R-component only if it appears alone. The velocities of V-subcomponents, when measured separately, are inclosed in parentheses. Additional fainter components, occasionally observed, are given in the notes appearing at the end of the table. As was mentioned previously, it is not possible to attach to the radial velocities a true measure of precision. However, from the intercomparison of the few duplicate observations made, we estimate that a radial velocity has a nominal probable error of 1 km/sec if measured on a 72-inch plate and of 3 km/sec for 36-inch plates. The agreement of our measures with those of Adams (1949) in the few stars we have in common is excellent, provided that the Adams velocities are increased by 1.5 km/sec to reduce them to the standard wave-length system.

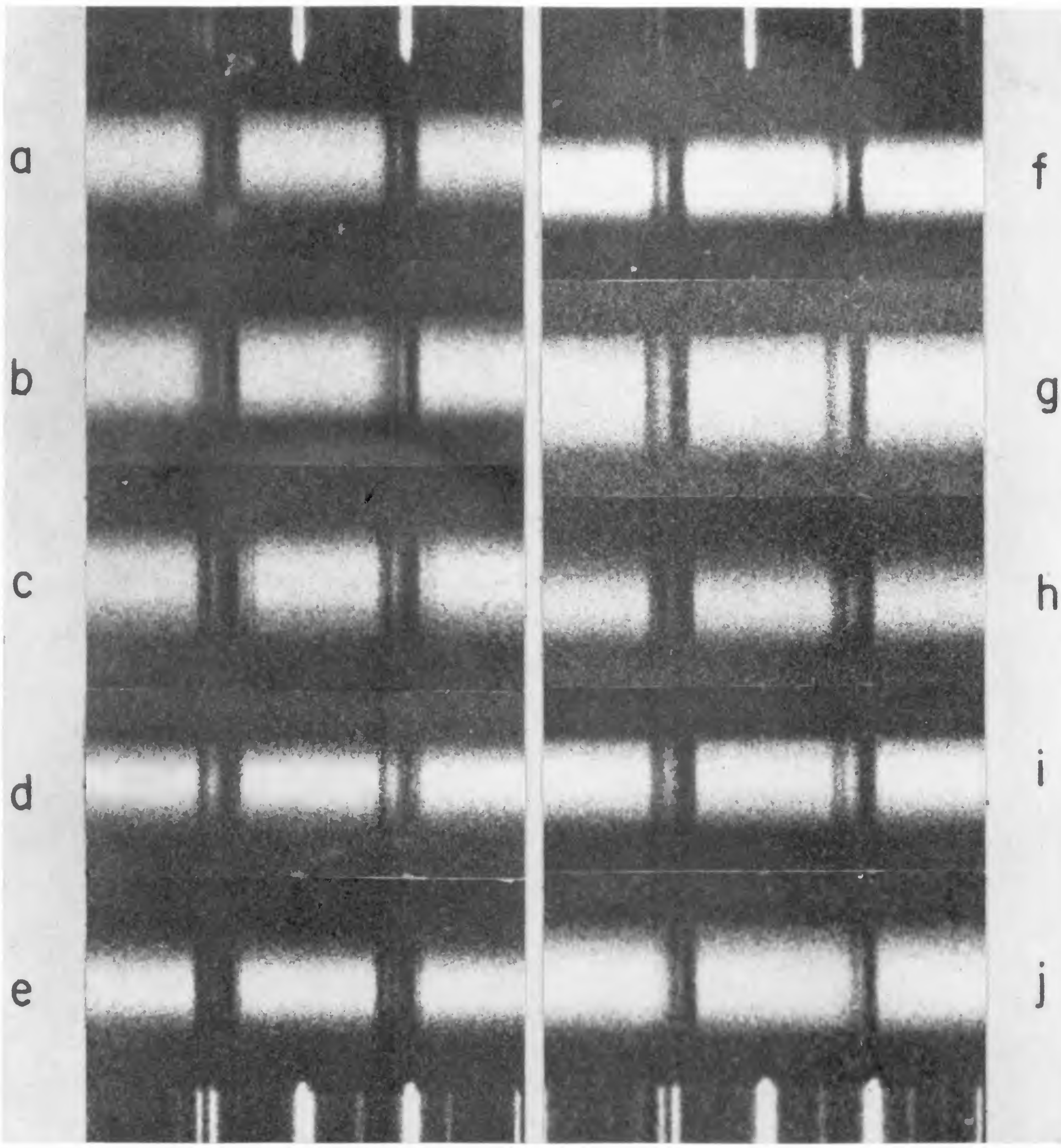

FIG. 1.—Interstellar Na I lines in stars of the Perseus spiral arm: *a*, HD 212455; *b*, HD 213470–1; *c*, HD 223385; *d*, HD 224055; *e*, HD 223960; *f*, HD 7902; *g*, HD 12953; *h*, HD 14134; *i*, HD 14143; and *j*, HD 14818. Dispersion of the originals 6.8 A/mm.

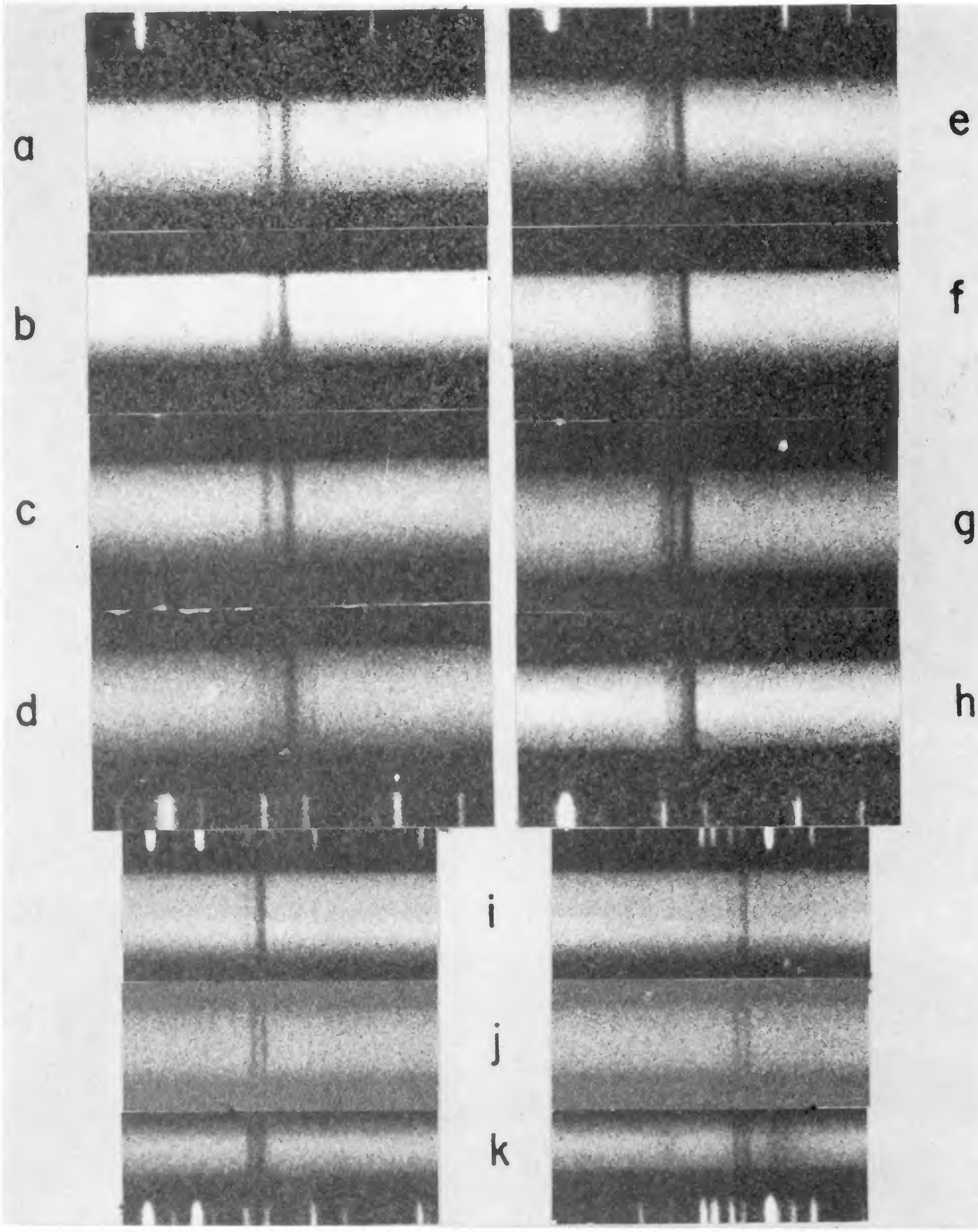

FIG. 2.—Interstellar Ca II lines in stars of the Perseus spiral arm. K line at 4.5 A/mm dispersion: *a*, HD 202124; *b*, HD 210809; *c*, HD 218915; *d*, 225094; *e*, HD 14134; *f*, HD 14143; *g*, HD 14818; and *h*, 17505. K (*right*) and H (*left*) lines at 9.2 A/mm dispersion: *i*, HD 1810; *j*, HD 14434; and *k*, HDE 237213.

b) Spectrophotometry

All plates obtained at Palomar were calibrated at the time of exposure, by means of a wedge spectrogram obtained with an auxiliary-grating spectrograph. At Mount Wilson the standard step-slits of the coudé (Williams 1934) were always used. Tracings on paper of the plates and the corresponding sensitometric marks were made in a microphotometer of the conventional transmission type, on a scale 216 times larger than the originals. Care was taken always to make the analyzing slit not wider than the narrowest iron comparison lines. A tracing of the D lines in a Pb plate of HD 223385 is reproduced in Figure 3, to give an idea of the quality of the basic photometric material. Intensity profiles were reduced point by point, after smoothing out the obvious noise caused by plate grain. The largest uncertainty in the estimates of percentage absorption arises from the placing of the "continuous" background, a problem which is most serious in the case of the H line in sharp-lined stars with Hϵ strong. In the case of cB stars, where the Hϵ line

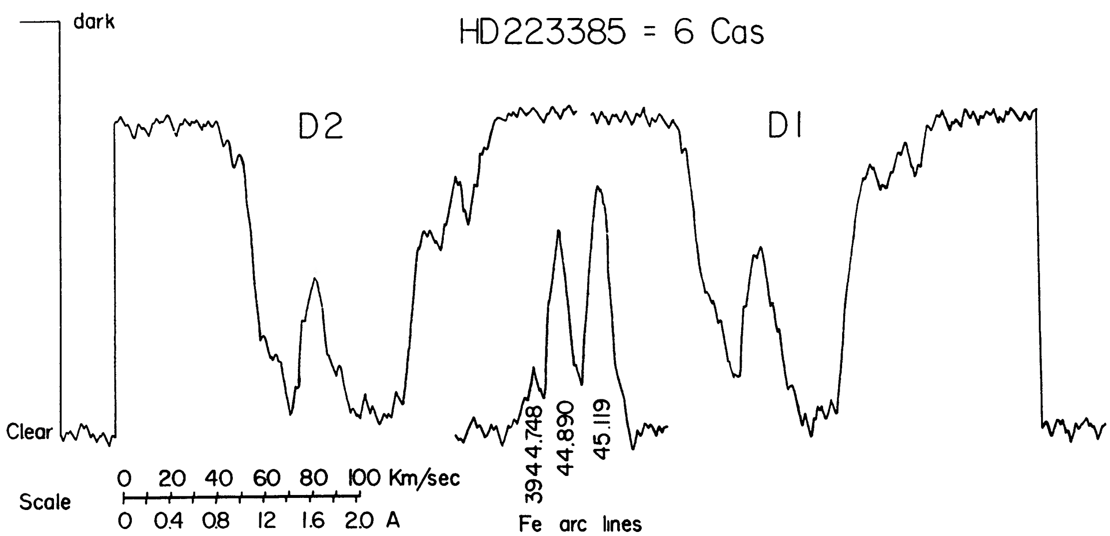

FIG. 3.—Non-linear microphotometer tracing of the interstellar Na II lines in HD 223385, from a second-order spectrum with 6 8 A/mm. The iron-arc comparison lines, reproduced to illustrate purity of spectrum, are from the third-order spectrum with 4 5 A/mm.

is not symmetrical, there is some arbitrariness in the drawing of the wing of Hϵ. However, since any kind of objective measure has more value than an eye-estimate, the procedure was carried out consistently for stars in each spectral class. Uncertainties arising from excessive grain or non-uniform background have led to the assignment of a low weight to the observation. In some D plates we have noticed an appreciable Eberhard effect, as the centers of the strong lines gave deflections beyond clear plate by amounts ranging up to 3 per cent of the dark-clear range. Although the uncertainty in the total intensity, resulting from placing the center of such lines at clear plate, is not large, we have given low weight to such observations. Plates developed in a rocking machine have not shown Eberhard effect to any appreciable extent. In Pb plates the width 2β of narrow comparison lines at half-peak intensity was measured to be in the mean 8.2 km/sec, with a standard deviation of ± 1 km/sec. For Pc plates 2β is twice as large.

The apparent separation of the R- and V-components in the complex profiles is large enough to permit an estimate of their individual intensities by means of a graphical procedure. The measured depths in a blended line were represented as the sum of the depths of two (or more) contours, drawn after considering the steepness of the instrumental profile and the shape of the line in its parts less affected by the blend. Samples of contours thus dissected are shown in Figure 4. The equivalent widths, W, of the components were then determined by graphical and/or numerical integration, referring them to the "continuous" background. They are given in the ninth and tenth columns of Table 1 in the same order as the velocities appear in the preceding column. When the velocities of two lines appear in parentheses, the equivalent width given refers to the blended feature. The degree of separation between two components has been measured by a digit number z appearing within parentheses between the W's of the respective components. If d_1 and

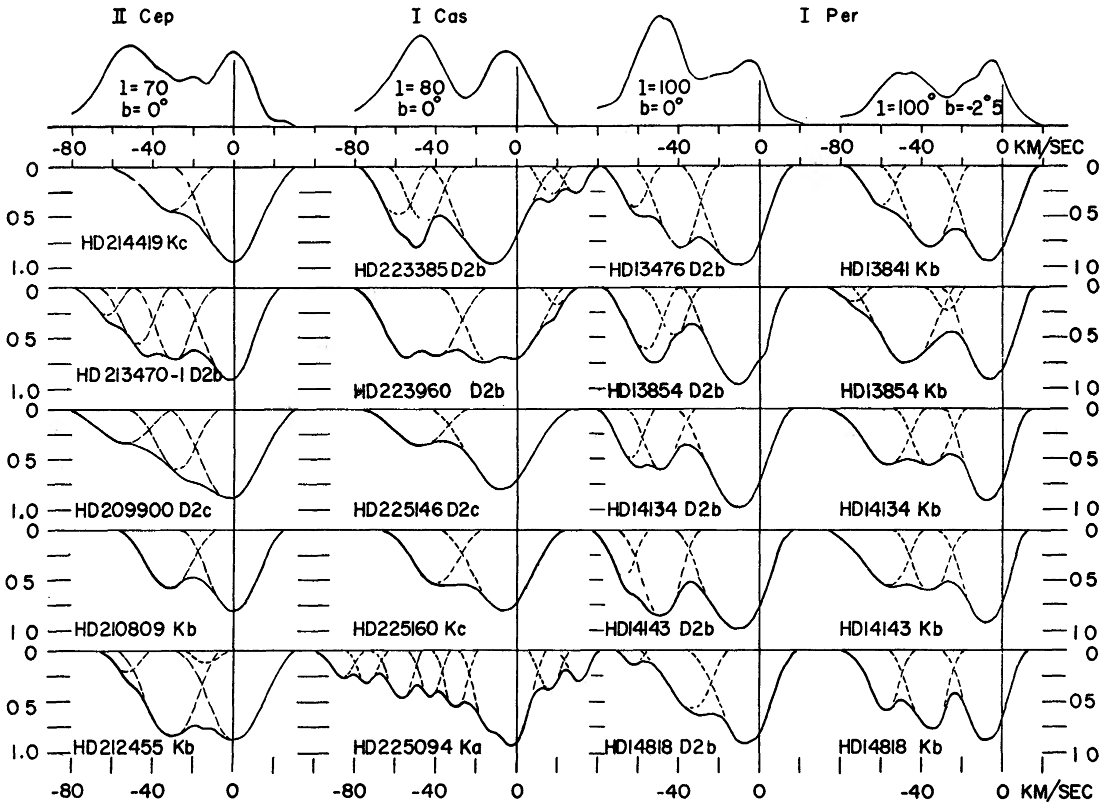

FIG. 4.—Profiles of interstellar lines in stars of the Perseus spiral arm. The abscissae represent radial velocities (km/sec) referred to local standard of rest, and the ordinates measure depths in units of the background continuum. For comparison purposes, at the top appear the contours of the 1420 mc/sec line of hydrogen at the position near the center of the associations indicated.

d_2 are the depths of the apparent centers of two blended components and d_{12} is the apparent depth at the point of maximum overlap, then we define

$$z = 10\left(1 - \frac{2d_{12}}{d_1 + d_2}\right). \qquad (1)$$

This number is thus similar to, but not identical with, the separation parameter used by Spitzer, Epstein, and Hen (1950). For weak components not measured separately from the main line, we have used the numeral "I" to indicate estimated equivalent widths less than 0.04 A for the stronger line of the doublet.

For interpreting the strengths of separate components it would be more meaningful to measure the equivalent width of the component formed closer to the observer in reference to the background determined by the other one. As will become apparent later, this would require the measurement of the intensity in the R line with reference to the contour of the V-component. On the basis of the material available, an attempt to carry out this reduction would lead to highly uncertain results. We have made, however, a rough estimate of the extent to which the W of the R-component may be affected on this account. Approximating one of the observed contours with $z = 3$ by two partially overlapping Gaussian curves of total strengths in the ratio 1:0.8 we found the W(R) increased by 12 per cent when referred to the background set by the weaker line. If the contour were corrected for instrumental broadening, z would increase to 5 and the W(R) would increase by only 7 per cent. Since actual contours have steeper wings than Gaussian curves with 20 km/sec half-width, the error affecting the W(R) is quite small. In comparison, we find, by repeated reductions of the same tracing, that the uncertainty introduced into W(R) or W(V) by the graphical dissection of a typical contour with $z = 3$ amounts to 10 per cent.

The over-all accuracy of the photometry is comparable to that of previous similar measures. From 16 pairs of plates we find a mean absolute deviation of 12 per cent for one total intensity. This figure is somewhat higher than that obtained by Spitzer *et al.* (1950) for Adams' plates, but not enough plates included in our comparison are of equally high quality to consider the difference significant. Comparing our total intensities with those obtained earlier at Mount Wilson (Merrill *et al.* 1937), we find no systematic differences, and the accidental scatter is compatible with the uncertainties of the individual determinations. Our intensities, like all previous Mount Wilson measures, differ systematically from those obtained at Victoria (Beals 1934, 1936; Beals and Oke 1953). The origin of this discrepancy, although much discussed in the past, remains obscure. It has been verified that the difference in the intensity scale is not due to the sensitometric calibration, nor can it be ascribed to internal characteristics of the spectrographs. The sample tracings and profiles reproduced in the paper by Beals and Oke (1953), however, definitely point to an instrumental effect as the origin of their large equivalent width. In Figures 2 and 3 of their paper a profile for the D lines in HD 14818 is given, showing "wings" extending about 200 km/sec from their centers. No data are given therein concerning the width of the instrumental contour, but, if it were 40 km/sec (amount equivalent to 25 μ projected slit width in 31 A/mm plates), no noticeable overlap should appear between D1 and D2, as both lines are deep, their separation is 300 km/sec, and their W's are of the order of 40 km/sec. It is instructive in this connection to compare the Victoria tracing of the D lines in HD 14818 with that published by Merrill *et al.* (1937) of the same lines in HD 14143, both obtained from plates of nearly the same dispersion. Although the lines in HD 14143 are stronger than in HD 14818, no overlapping at all between the two D lines appears in the Mount Wilson tracing. The spurious broadening of the Victoria line profiles may have been introduced into the microphotometer tracing by the use of an analyzing slit broader than the resolving power of the plate. The use of a wide analyzing slit may lead to spuriously large equivalent widths, as Cayrel (1953) and Deutsch (1954) have shown for the case of lines falling within the density range covered by the "linear" part of the characteristic curve of the plate. Strong interstellar lines are so deep and narrow that they often extend beyond the linear density range, but it may be proved that the increase in equivalent width for absorption lines traced with a wide slit holds in general. We shall not attempt now to evaluate the errors affecting the Victoria photometry on this account, as most of the data required are not available in published form. It would appear reasonable, however, to consider the Victoria results for the time being as more likely to be in error than the Mount Wilson measures.

IV. ANALYSIS OF THE RADIAL VELOCITIES

a) *Structure of the Lines*

Let us consider, first, the structure of the interstellar lines listed in Table 1, in relation to the position of the stars in which they appear. In Figure 5 we exhibit the dependence on distance and galactic longitude of the radial velocities of the V- and R-components, referred to the local standard of rest. The values represented are denoted by dots or circles, depending on whether the distance modulus of the star concerned is larger or smaller than 11.0. A division into such nearby and distant groups is quite natural, since very few high-luminosity early-type stars are found with distances between 1 and 2 kpc. For reasons of clarity we have omitted from the diagram components either with positive displacements or with intensities given as I. Multiple V-components, moreover, have been represented by a single point referring to the mean velocity. Data related to stars in a recognized association have been grouped into average values, identified in Figure 5 by larger-sized symbols. The range in velocity covered by multiple V-components in the association is indicated by the length of segments drawn through the mean values. For reference purposes we have plotted the radial velocities of the distant stars observed, corrected for local solar motion, and also the galactic-rotation-curves for the

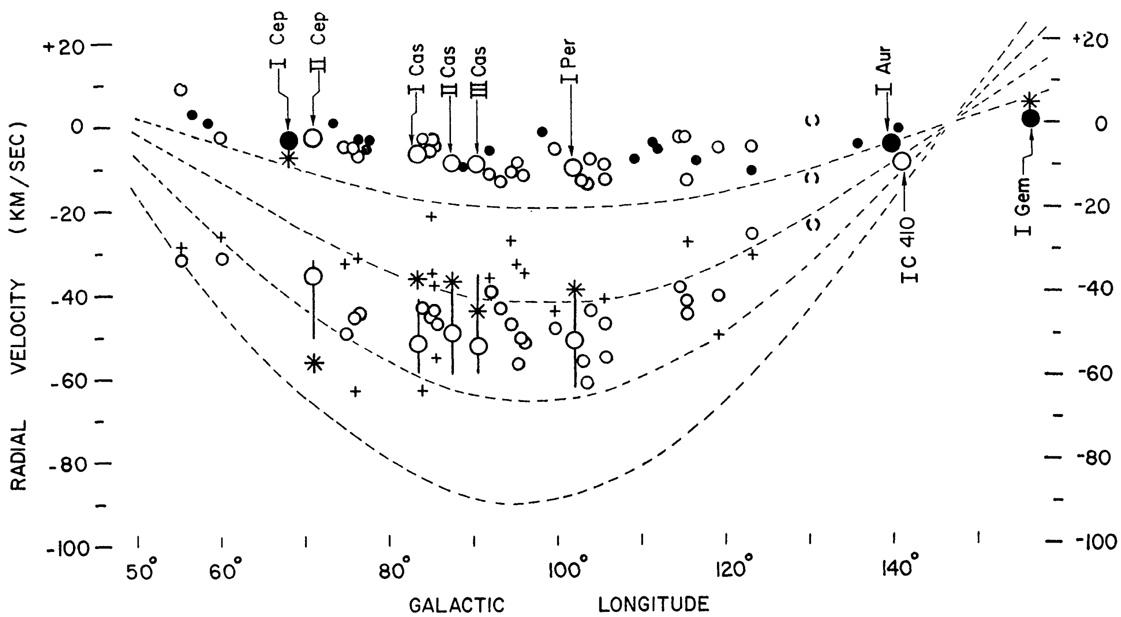

FIG. 5 —The dependence on galactic longitude (*abscissae*) of the radial velocities in the local standard of rest (*ordinates*) of the strong components of interstellar lines in the northern Milky Way Dots refer to stars in the Orion spiral arm; circles to stars in the Perseus arm. Larger-sized symbols represent O associations. The star BD+43°1168 at $l = 130°$ has been entered with a special symbol, to indicate that the separation of the two components is marginal The radial velocities of the distant stars are represented by + signs, while those of the O associations are denoted by *. The broken-line curves represent the galactic-rotation effect on the radial velocities of points at distances of 1, 2, 3, and 4 kpc.

radial motion of points at distances $r = 1, 2, 3$, and 4 kpc from the sun. They were computed from the expression

$$V_r = R_0 [\omega(R) - \omega(R_0)] \sin l' , \tag{2}$$

where R and R_0 are the distances to the galactic center of the point considered and of the sun, respectively; l' is the galactic longitude measured from the center; and $\omega(R)$ is the angular velocity of the system. The numerical values of the parameters involved have been taken from van de Hulst *et al.* (1954).

The general arrangement of the points in Figure 5 shows clearly that the velocities of the interstellar lines in the nearby group of stars, together with the R-components in distant ones, follow quite well the galactic-rotation-curve of a point at a distance of about 0.5 kpc. The V-components, on the other hand, correspond to galactic-rotation shifts of points at distances between 2 and 3 kpc. The general arguments justifying the interpretation of the radial velocities of the V-components as an effect of differential motion have been advanced earlier (Münch 1953). The more extensive observations here presented establish, in a still clearer fashion, the dependence on longitude of the separation between the R- and V-components: the three stars in IC 410, at a distance of 3.6 kpc toward the anticenter (Sharpless 1955), show strong lines with no trace of being double, while HDE 232999 at $l = 123°$ distinctly shows the double lines, and in BD+43°1168 at $l = 130_0$ the lines are broad enough to suggest strongly incipient resolution. After passing through a broad maximum around $l = 100°$, the separation again decreases as the direction of galactic rotation is approached. The radial velocities of the V-components, on the other hand, are always quite close to those of the stars in which they are observed, if a small but noticeable systematic difference is disregarded for the time being. There can be no doubt, then, that the V-components are formed in the immediate surroundings of the distant stars and that, in directions around $l = 100°$, the mean space density of the interstellar gas at distances between 1 and 2 kpc is considerably lower than outside this range. Confirming our preliminary results, we thus verify that the interstellar gas clouds are strongly concentrated along the structural features of the galactic system outlined by the H II regions (Morgan *et al.* 1952) and the O associations (Morgan *et al.* 1953). Following the terminology suggested by van de Hulst *et al.* (1954), we shall refer to the nearby feature as the "Orion spiral arm" and to the more distant one as the "Perseus arm."

It has been mentioned that the radial velocities of the V-components seem to be systematically shifted with respect to those of the distant stars. The effect is most convincingly shown by the mean values referring to the associations, where peculiar motions and observational uncertainties play a smaller role. In the case of I Per and I, II, and III Cas, the V-components are displaced by about −12 km/sec with respect to them. Only for the association II Cep, is the difference of opposite sign, amounting to 20 km/sec. It might be questioned whether for this purpose it is appropriate to compare the mean values of the V-components. An inspection of the contours reproduced in Figure 4 shows that the V-components vary appreciably from star to star in the same association, indicating that the density and motion of the gas change appreciably within the volumes of space considered. It is difficult to attach a precise meaning, under these conditions, to a formal average of the radial velocities, formed by disregarding the positions of the points involved and the relative intensities of the line components. We may notice, however, that the mean radial velocities of the V1 components for I, II, and III Cas and I Per are equal to those of the respective associations within 3 km/sec. The question now becomes why in these cases we also observe interstellar-line components shifted systematically to the violet, with respect to the standard of rest of the association, by amounts of the order of 20 km/sec. The most direct explanation we may advance is in terms of a general expansion tendency of the interstellar gas surrounding large O associations. In the solar neighborhood, systematic motions of the kind have been detected in the case of I Ori (Merrill and Sanford 1938; Adams 1949) and II Per (Blaauw 1952). Furthermore, on the basis of ideas currently held for the origin of the acceleration of interstellar gas clouds (Kahn 1954; Oort 1954; Oort and Spitzer 1955; Savedoff and Greene 1955), the expanding tendency we have observed is readily understood. The case of II Cep, we might say, is an exception, since it is a very distant group of stars ($r = 3.6$ kpc). The possibility of accounting for the apparent motion between this association and the interstellar-line components as an effect of galactic rotation is indeed quite likely. As we shall see, toward $l = 70°$ the observations of the 21-cm hydrogen line seem to indicate branching of the Perseus arm. It may be remarked, moreover, that the absence of lines clearly indicating large-scale expansion around II Cep is not an argument against the explanation offered here for the other O associations. For it would seem apparent that the existence and extent of the expansion will depend sensitively on a variety of conditions not necessarily satisfied around every O association.

b) Comparison with the 21-Cm Hydrogen Line

The 1420 Mc/sec emission line of hydrogen provides information regarding the density and velocity of the gas within the acceptance cone of the antenna used in its observation. At the distance of the Perseus arm, currently employed antennae, such as that used by the Dutch astronomers (van de Hulst *et al.* 1954), have acceptance cones with cross-section diameters of the order of 100 pc. Keeping in mind the entirely different order of magnitude of the volumes of space in which the 21-cm and the optical lines arise, we now compare their profiles. In figure 4 we have reproduced the profiles of the 21-cm line observed in the Netherlands, kindly provided by Professor Oort in advance of publication, at the positions of O associations. On the whole, the agreement between the positions of the maxima of the 21-cm line and of the deepest points in our absorption contours is quite satisfactory. The velocity of the component arising in the Orion arm is essentially the same whether derived from the radio or from the optical observations. In fact, the agreement is so good that we may interpret it as indicating that the Na I and Ca II lines we have observed must arise predominantly in H I regions. The lines arising in the Perseus arm show differences which, on the basis of the remarks made at the beginning of this paragraph, are not difficult to explain. At the position of II Cep the hydrogen line in the Perseus arm has its main maximum at -52 km/sec, and it is extended to longer wave lengths, with secondary maxima at -35 and -20 km/sec. All our stars in that association show a component near -35 km/sec and some of them also components around -50 km/sec (e.g., HD 213470–1, HD 209900, and HD 212455). It is apparent, thus, that some of the optical components arise at closer distances from the sun than the main concentration of interstellar gas in this direction. In the case of the other four distant associations (only two of them included in Fig. 4), the position of the 21-cm maximum agrees well with the mean position of the optical V-components. Since undoubtedly these associations are not so distant as the regions of maximum gas density in the Perseus arm, the smaller distance of the gas producing the optical components is not shown by their mean velocities because of the expanding gas around these associations as we discussed before.

It is of interest to emphasize the variations of the optical lines in associations, in contrast to the smooth form of the 21-cm line and the slow manner in which it changes as the observed direction changes. It signifies, as the radio astronomers conjectured, that the 21-cm line refers to a volume of space large enough to contain many gas clouds. Such statistical stability of the 21-cm-line profiles observed with today's antennae greatly simplifies the derivation of the large-scale features in the space arrangement of the interstellar gas. At the same time, it obliterates significant features in the velocity distribution of the interstellar gas clouds, in spite of the fact that the resolving power in frequency of the radio observations compares with, or may be greater than, that of the optical ones. For example, we may refer to the striking complexity of the optical lines in the region around $l = 85°$, which is not at all apparent in the 21-cm profiles. The derivation of the space densities of interstellar hydrogen by van de Hulst *et al.* (1954) is based on the assumption that the velocity distribution of the gas clouds is everywhere the same as that derived from the optical lines observed in nearby stars (Blaauw 1952). These authors realized that the weakest link in the reductions is the correction for random mass motions of the clouds; and, indeed, in order not to obtain "negative densities" at some points, they have diminished the width of the adopted velocity distribution to make the density of gas at most just vanish. But they did not have the means to find out whether in some regions the velocity distribution was wider than the adopted one. The appearance of their Figure 16 showing the mean space density of hydrogen in the neighborhood of the sun, however, strongly suggests that the random motions are not the same in different directions or even at different distances along the same line of sight. For most of the smaller-scale features in the tentative density distribution of interstellar hydrogen show an obvious symmetry with respect to the observer which undoubtedly is not real. Future analysis of 21-cm-line data derived with the aid of much larger antennae may provide information about the velocity distribution of the clouds as a function of position. For the time being, however, some caution should be exercised in interpreting minor details present in 21-cm-line profiles as a feature in the space arrangement of hydrogen atoms.

V. ANALYSIS OF THE LINE INTENSITIES

a) Curves of Growth

We shall analyze the equivalent widths listed in Table 1 following the "doublet ratio" method, originally developed by Wilson and Merrill (1937). If the probability law, $\psi(v)$, of the radial velocities of the atoms forming a line doublet (such as K and H or D2 and D1) is known, then the doublet ratios K/H or D2/D1 and the equivalent widths are completely determined by the total number of atoms, N, in a column of unit cross-section along the line of sight. For the case when $\psi(v)$ is Gaussian with a standard deviation b,

$$\psi(v) = \frac{1}{b\sqrt{\pi}} e^{-(v-v_0)^2/b^2}, \tag{3}$$

and v_0 is independent of distance, Strömgren (1948) has evaluated the intensities W and the doublet ratios as functions of N and b. Strictly speaking, equation (3) applies only to thermal motions, which in the case of interstellar atoms are much smaller than their mass motions. But, in an approximate fashion, it also applies to a situation in which the line arises in a number of turbulent elements with a Maxwellian velocity distribution, provided that the line formed in each of them is unsaturated and much narrower than the total line width. The differential motion of the local standards of rest along the line of sight may be taken into account (Jentzsch and Unsöld 1948) if the absorbing atoms are supposed to be distributed uniformly in space. For stars confined to the Orion spiral arm, where the assumption of uniformity is satisfied fairly well, the effect of galactic rotation on the line intensities is negligible, as we shall show later. The intensities of lines with components formed in two spiral arms are affected significantly by galactic rotation, but to assume a uniform distribution is quite unrealistic. In such cases the intensities and doublet ratios of the two components may be analyzed separately, neglecting within each arm the effect of differential rotation.

The representation of the turbulent velocities of the interstellar gas by a Gaussian law, as in equation (3), has hardly any theoretical or observational basis. It is true that in the laboratory it has been verified that the energy-containing eddies of incompressible turbulent flows have velocities distributed nearly according to the normal law (Batchelor 1953). But the same will not necessarily hold true in supersonic turbulence, for the increased dissipation by pressure waves (Lighthill 1955) will tend to make the velocity distribution flatter than a Gaussian law. On the observational side, it has been found (Blaauw 1952) that a law of the form

$$\psi(v) = \frac{1}{2\eta} e^{-|v-v_0|/\eta} \qquad (\eta = \text{Const}) \tag{4}$$

represents more closely the observed frequencies of occurrence of interstellar lines with radial velocities v than does equation (3). Also the 21-cm-line profiles (van de Hulst *et al.* 1954) give indication of the existence of a long tail in the velocity distribution of the interstellar gas, as is predicted by equation (4). It is a matter of interest, therefore, to inquire about the shape of a curve of growth of an absorption line formed in gas elements moving according to the law symbolized in equation (4).

Let W be the equivalent width of a line with transition probability a_{k1} arising between two energy states with statistical weights g_k and g_1. The fictitious optical depth at the center of the line for the case of a velocity distribution of type (4) is

$$\tau_0 = \frac{\lambda_0^4}{16\pi c} \frac{g_\kappa}{g_1} a_{k1} \frac{N}{\eta_\lambda}, \tag{5}$$

where λ_0 is the rest wave length of the line and η_λ is the Doppler width,

$$\eta_\lambda = \frac{\lambda_0}{c} \eta . \tag{6}$$

If damping is neglected, it may be readily shown that

$$\frac{1}{2\eta_\lambda} W(\tau_0) = \ln \gamma \tau_0 + E_1(\tau_0), \tag{7}$$

where $\ln \gamma = 0.5772 \ldots$ is Euler's constant and $E_1(\tau_0)$ is the first exponential integral. The limiting behavior of equation (7) is described by the power series,

$$\frac{1}{2\eta_\lambda} W(\tau_0) = \sum_{n=1}^{\infty} (-1)^n \frac{\tau_0^n}{n!n}, \tag{8}$$

and the asymptotic expansion,

$$\frac{1}{2\eta_\lambda} W(\tau_0) = \ln \gamma \tau_0 + e^{-\tau_0} \sum_{n=0}^{m} (-1)^n \frac{n!}{\tau_0^{n+1}} \qquad (\tau_0 \to \infty). \tag{9}$$

Suppose τ_0 refers to the fainter line of the Ca II or Na I resonance doublet. The equivalent width of the stronger line then is $W(2\tau_0)$, and the value of the doublet ratio is

$$DR = \frac{\ln 2\gamma \tau_0 + E_1(2\tau_0)}{\ln \gamma \tau_0 + E_1(\tau_0)}. \tag{10}$$

The numerical dependence on τ_0 of DR and $\log_{10} W/\eta_\lambda$ predicted by equations (7) and (10) is given in Table 2. An observed value of DR fixes the corresponding values of τ_0

TABLE 2

CURVE OF GROWTH FOR AN EXPONENTIAL VELOCITY LAW

$\log \tau_0$	DR	$\log W/\eta_\lambda$	$\log \tau_0$	DR	$\log W/\eta_\lambda$
−1 0	1 95	−0 71	+0 6	1 35	0 60
−0 8	1 92	− 52	+0 8	1 29	0 68
−0 6	1 88	− 33	+1 0	1 24	0 76
−0 4	1 83	− .14	+1 2	1 20	0 82
−0 2	1 75	+ 04	+1 4	1 18	0 88
0	1 66	+ 20	+1 6	1 16	0.93
+0 2	1 55	+ 35	+1 8	1 14	0 97
+0 4	1 44	+0 48	+2 0	1 13	1 02

and W/η_λ. The observed W then determines η_λ immediately, and from equation (5), rewritten in the form

$$\frac{\tau_0}{W/\eta_\lambda} = \frac{\lambda_0^4}{16\pi c} \frac{g_k}{g_1} a_{k1} \frac{N}{W}, \tag{11}$$

we evaluate N. Introducing in equation (11) the numerical values of the atomic parameters involved, we find

$$\log N(\text{Na I}) = 13.27 + \log W + \log \tau_0 - \log \frac{W}{\eta_\lambda}, \tag{12}$$

$$\log N(\text{Ca II}) = 13.60 + \log W + \log \tau_0 - \log \frac{W}{\eta_\lambda}. \tag{13}$$

For τ_0 sufficiently large, the exponential terms in equations (7) and (10) may be neglected, and we have simply

$$\frac{1}{2\eta_\lambda} W(\tau_0) = \ln \gamma \tau_0 \quad \text{and} \quad DR = \frac{\ln 2\gamma\tau_0}{\ln \gamma\tau_0}. \tag{14}$$

The error introduced into equation (7) by neglecting $E_1(\tau_0)$ is about 4 per cent for $\tau_0 = 2$, while for $\tau_0 = 3$ it is less than 1 per cent. From equations (14) it follows that

$$\eta_\lambda = \frac{DR - 1}{\ln 4} W(\tau_0) = 0.7213\,[W(2\tau_0) - W(\tau_0)]. \tag{15}$$

Expressing η in kilometers per second and the equivalent widths in angstroms, we have, from equation (15),

$$\eta_{\text{Na I}} = 36.7\,(\text{D}2 - \text{D}1), \tag{16}$$

$$\eta_{\text{Ca II}} = 54.7\,(\text{K} - \text{H}). \tag{17}$$

It is of interest to notice that, as $\tau_0 \to \infty$, η as given by equation (15) and b as given by the asymptotic expansion for W/b corresponding to a Gaussian distribution obey the relation

$$\frac{b}{\eta} = \left(\frac{\ln 4}{DR - 1}\right)^{1/2}. \tag{18}$$

The asymptotic forms of equations (12) and (13) are

$$\log N(\text{Na I}) = 12.88 + 0.301 \frac{\text{D}1}{\text{D}2 - \text{D}1} + \log(\text{D}2 - \text{D}1), \tag{19}$$

$$\log N(\text{Ca II}) = 13.21 + 0.301 \frac{\text{H}}{\text{K} - \text{H}} + \log(\text{K} - \text{H}). \tag{20}$$

b) D Lines in the Orion Arm

It was pointed out by Wilson and Merrill (1937) that the observed values of D2/D1 decrease from 2.0 to about 1.2 as D2 increases from zero to about 0.5 A and that, as D2 increases further, D2/D1 remains sensibly constant. On this basis they suggested the existence of large inhomogeneities in the spatial distribution of the interstellar sodium, having a linear scale of the order of 700 pc. Later analysis of the same observational material did not investigate further the suggestion of Wilson and Merrill and, instead, searched for alternative explanations, generally postulating a uniform distribution of the gas in space. In particular, Jentzsch and Unsöld (1948) showed that the observed doublet-ratio-curves can be explained if the root-mean-square velocity of mass motion V_D of the gas, if distributed according to equation (3), increases in all directions as the distance from the sun increases. In view of the far-reaching consequences of the Jentzsch and Unsöld conclusions, it is of importance to reconsider the problem, incorporating the results of our observations.

We begin by noticing that, among the forty-six stars given in the Mount Wilson catalogue of interstellar-line intensities (Merrill *et al.* 1937) as having $\frac{1}{2}(\mathrm{D2} + \mathrm{D1}) > 0.5$ A, thirty-two are located in the Perseus arm. Thus their interstellar lines cannot be analyzed on the assumption of a uniform distribution of the gas along the line of sight. In order to include in the analysis only stars within the Orion arm, only those for which $\mathrm{D2} < 0.5$ A should be considered. Still, with this limitation on D2, a significant increase in V_D with D2 is apparent, as may be seen in Table 3, the first five columns of which have been taken from Jentzsch and Unsöld (1948). If the same mean values of D1 and D2/D1 are analyzed with the aid of Strömgren's tables (1948), the values of b and N given in the sixth and seventh columns are obtained. We notice that the values of b are only slightly larger than V_D, an indication that galactic rotation plays only a minor role in determining the line intensity at these small distances. On the other hand, if we analyze the same values of D1 and D2/D1 by means of the curve of growth given in Table 2, the values of $\eta\sqrt{2}$ (root-mean-square velocity) and N appearing in the last two columns of Table 3 result. Unlike the values of V_D or b, those of $\eta\sqrt{2}$ do not show any significant variation over the intensity range of D1 considered, and the constant value $\eta\sqrt{2} = 4.6$ km/sec is well determined. If galactic rotation were taken into account, $\eta\sqrt{2}$ would

TABLE 3

MEAN D-LINE INTENSITIES IN THE ORION ARM

D2		D2/D1	V_D (km/sec)	log N	b (km/sec)	log N	$\eta\sqrt{2}$ (km/sec)	log N
A	km/sec							
0.05	2 55	1 90	3 2	11 5	6 7	11 5	4 8	11 4
10	5 10	1 80	4 8	11 8	5 6	11 8	4 7	11 8
15	7 05	1 71	5 8	12 0	6 0	12 0	4 8	12 0
20	10 2	1 61	6 1	12 2	6 0	12 2	4 8	12 3
30	15 3	1 42	6 2	12 5	6 6	12 5	4 7	12 5
40	20 4	1 28	6 9	12 8	6 7	12 8	4 2	12 9
0 50	25 5	1 22	7 7	13 0	8 0	13 0	4 8	13 2

decrease by an amount of the same order as the difference $b - V_D$ corresponding to the same value of D1. The results of the calculation summarized in Table 3 are represented graphically in Figures 6 and 7, where the loci of constant N and constant η (Fig. 6) or constant b (Fig. 7) are drawn in (D1, D2/D1) co-ordinates. The position of Jentzsch and Unsöld normal points in Figure 6 is seen to follow the general trend of the curves η = Constant, while in Figure 7 they definitely cut across the loci of constant b. Thus we may conclude that the mean intensities of the D lines in stars of the Orion arm can be interpreted in terms of a velocity distribution resembling equation (4), with a constant root-mean-square velocity $\eta\sqrt{2} = 4.6$ km/sec. It is conjectured that if the effects of galactic rotation were taken into account, the velocity distribution (4) would predict a slight excess of high velocities.

Our measurements of the R-components of the D lines in distant stars may also be analyzed by the method followed above. These lines are so saturated, however, that the observational errors affecting individual values of D2 and D1 make the determination of N and η (or b) quite uncertain. It is thus convenient to form normal points from the individual measures in groups of stars relatively close in space. The straight averages of the R-components of the D lines observed in stars in and near the associations have been formed, with the results given in Table 4. The calculation of weighted means does not lead to significantly different values, nor does the manner in which the mean doublet ratio is formed, as it may be seen from the nearly identical values of $\langle \mathrm{D2} \rangle / \langle \mathrm{D1} \rangle$ and

$\langle D2/D1\rangle$. The corresponding normal values of $\eta\sqrt{2}$ and log N derived from equations (16) and (19) are also given in Table 4, together with the value of b obtained from equation (18). It may now be seen in Table 4 and also in Figures 6 and 7 that the mean intensities of the D lines formed in the whole width of the Orion arm lead to values of η and b which follow the general trend established by the points representing the intensities in the nearer stars within the Orion arm.

c) D Lines in the Perseus Arm

It has been shown in Section IV*a* that the interstellar gas around the large associations in the Perseus arm has a systematic motion of expansion revealed by line components with velocities negative with respect to the associations. It is thus not proper to

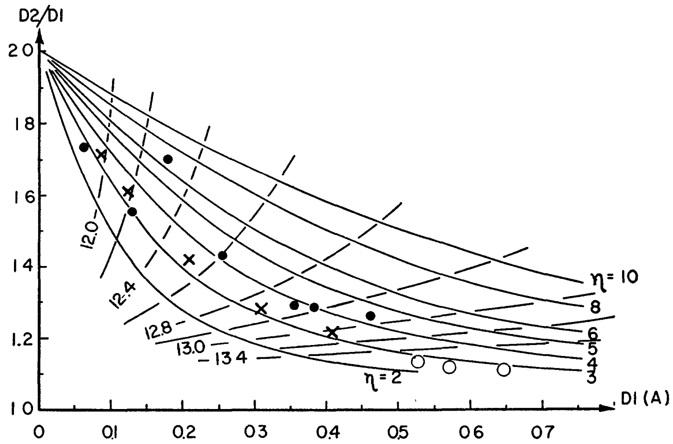

FIG 6 —Doublet-ratio-curves of the Na I lines for an exponential velocity law of mean speed η. The solid lines represent the loci of constant η and are labeled at their right ends by the value of η in km/sec. The broken lines represent loci of constant number of atoms along the line of sight, N, and are labeled at their left ends by the values of log N The empty circles denote observed mean values in the Orion arm; the dots refer to observed values in the Perseus arm; and the $\times$ symbols represent mean values for nearby stars

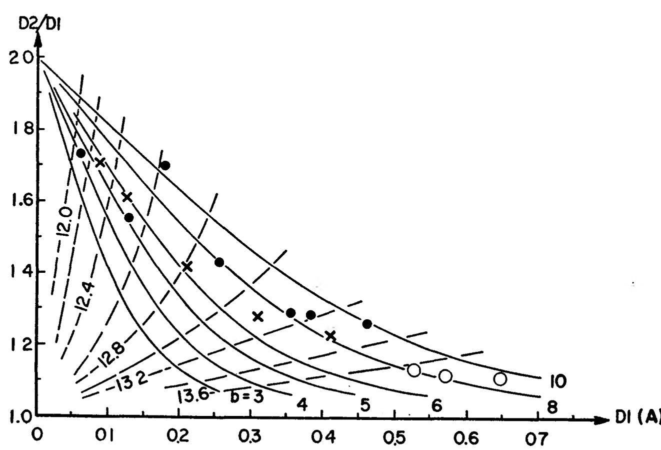

FIG 7 —Doublet-ratio-curves of the Na I lines for a Gaussian velocity law of dispersion b. The solid lines represent the loci of constant b and are labeled at their right ends by the value of b in km/sec. The broken lines represent loci of constant number of atoms along the line of sight, N, and are labeled at their left ends by the values of log N. The empty circles denote observed mean values in the Orion arm; the dots refer to observed values in the Perseus arm; and the $\times$ symbols represent mean values for nearby stars.

analyze the intensities of the lines arising in the Perseus arm by the doublet-ratio method, since their components do not have motions strictly at random. In a formal fashion, however, we may obtain values of N and η (or b) which should be understood as if they had been derived from line intensities measured, say, on the Pc plates, where the V-components appear unresolved. In order to minimize the errors of measurement, we consider the normal points formed only from the line intensities of high weight. Considering stars in and near the distant associations with line intensities approximately equal, we have found the mean values D1 and D2/D1 given in Table 5. The analysis of these normal values by the curve of growth given in Table 2 leads to the values of $\eta\sqrt{2}$ and log N appearing in the last two columns of Table 5. It may be seen here and also in Figure 6

TABLE 4

MEAN INTENSITIES OF D LINES FORMED THROUGH THE ORION ARM

Normal	l	No. of Stars	⟨D1⟩ (mA)	⟨D2⟩/⟨D1⟩	⟨D2/D1⟩	$\eta\sqrt{2}$ (km/sec)	log N	b (km/sec)
(16) II Cep, (16) I Cas	70°– 85°	6	524	1 134	1 138	3 6	13 9	8 2
(20) III Cas	90°– 95°	6	646	1 115	1 113	3 8	14 4	9 4
(21) I Per	100°–103°	8	570	1 119	1 119	3 5	14 2	8 4

TABLE 5

MEAN D-LINE INTENSITIES IN THE PERSEUS ARM

Normal	No. of Stars	D1 (mA)	D2/D1	$\eta\sqrt{2}$ (km/sec)	log N
(16) II Cep	2	468	1 25	6 2	13 2
(18) I Cas	3	184	1 70	8 1	12 2
(20) III Cas	3	65	1 76	4 5	11 8
(21) I Per	4	162	1 66	7 4	12 3
	5	258	1 42	5 7	12 5
	2	382	1 28	5 7	13 0

that the values of $\eta\sqrt{2}$ are larger than those obtained for the Orion arm stars by factors between 1.2 and 1.5.

d) Ca II *Lines in the Orion Arm*

The results of analysis of the Ca II lines by the doublet-ratio method are less precise than those provided by the Na I lines because of the difficulty involved in obtaining reliable intensities for the hydrogen line. Measures of the hydrogen line made with different dispersions not only show larger scatter around a mean than do other strong interstellar lines but also undoubtedly are affected by systematic errors. This is shown clearly by comparing the mean values of K/H obtained by Sanford and Wilson (1939) with those compiled by Binnendijk (1952) from various sources. We have formed mean values of K/H for given H from the measures by Spitzer *et al.* (1950) of stars in the Orion arm and found them definitely smaller than those of Sanford and Wilson (1939) and in accordance with Binnendijk (1952). This agreement indicates only that the averaging procedure is meaningful, but, in view of the larger extent and increased dispersion of the later observational material, it is reasonable to consider it as more likely to be free of error.

In Figures 7 and 8 we have plotted the normal points (K/H, H) adopted by Binnendijk (1952) and also those analyzed by Jentzsch and Unsöld (1948), which are based on the work of Sanford and Wilson (1939). With reference to the curves of constant η, which have been drawn in Figure 7, it is seen that those mean values of K/H considered to be more accurate follow quite well the locus η = 6 km/sec, while the points based on earlier work would correspond to η = 12 km/sec. As was found in Section V*b* for the Na I lines, in Figure 8 we may see that the mean points of K/H in the Orion arm do not follow the general trend of the curves *b* = Constant but would indicate an increase in *b* with distance from the sun.

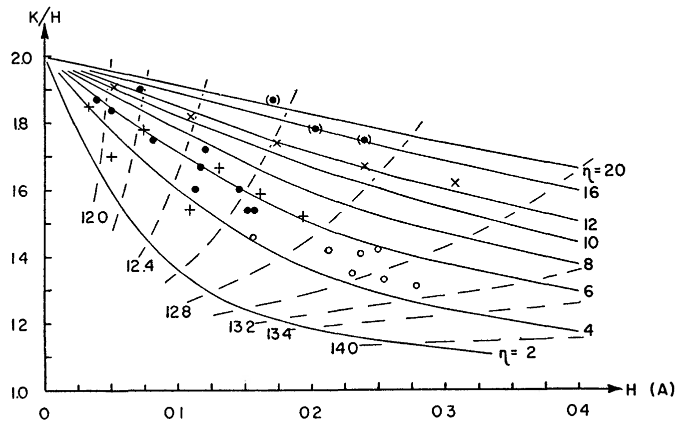

FIG. 8.—Doublet-ratio-curves of the Ca II lines for an exponential velocity law of mean speed η. The solid lines represent the loci of constant η and are labeled at their right ends by the value of η in km/sec. The broken lines represent loci of constant number of atoms along the line of sight, N, and are labeled at their left ends by the values of log N. The empty circles represent observed mean values in the Orion arm; the dots refer to observed values in the Perseus arm, with the three inclosed in parentheses representing stars in h and χ Persei; the + signs denote mean values as given by Binnendijk, while the × signs are the mean values adopted by Jentzsch and Unsöld.

TABLE 6

MEAN INTENSITIES OF THE Ca II LINES FORMED IN THE ORION ARM

Normal	No. of Stars	⟨K⟩ (mA)	⟨H⟩ (mA)	⟨K⟩/⟨H⟩	$\eta\sqrt{2}$ (km/sec)	log N	b (km/sec)
(15) I Cep	5	227	156	1 46	5 9	12 7	9 4
(16) II Cep	4	334	236	1 41	7 5	12 9	10 5
(18) I Cas	3	339	254	1 33	6 8	13 0	9 8
(19) II Cas	5	349	250	1 40	7 8	13 0	11 3
(21) I Per	7	310	230	1 35	6 7	13 0	9 2
(25) I Gem	5	303	213	1 42	7 0	12 9	10 1
IC 410	3	366	279	1 31	6 8	13 1	10 3

Our measurements of the Ca II components observed in distant stars as being formed in the Orion arm will be shown now to be in essential agreement with the conclusions derived in the preceding paragraph. In Table 6 are listed the mean intensities of the H and K lines or components formed in the Orion arm, in some of the associations. In the calculation of the averages, only stars with spectral types earlier than B2 and with line intensities with high weight have been included. The application of the curve of growth given in Table 2 to these normal points leads to values of η and log N as given in the sixth and seventh columns of Table 6, while the values of b appearing in the eighth column result from Strömgren's curve of growth. It may be seen now that the value $\eta = 6$ km/sec found before for stars within the Orion arm also represents satisfactorily the intensities of the Ca II lines formed through the whole width of the Orion arm.

e) Ca II *Lines in the Perseus Arm*

In the same manner as the V-components of the D lines were analyzed in Section V*c*, we now proceed to consider the doublet ratio of the Ca II lines formed in the Perseus arm. In view of the limited number of distant stars in Table 1 with reliable Ca II line intensities (free of possible blend with stellar lines), we have not formed normal points, and, instead, we consider simply the individual observations of high weight. The results of the analysis are presented only in graphical form in Figures 8 and 9, where it may be noticed that, in general, there appears no tendency for the (K/H, H) points in the Perseus arm to fall above or below the doublet-ratio-curve defined by the lines in the

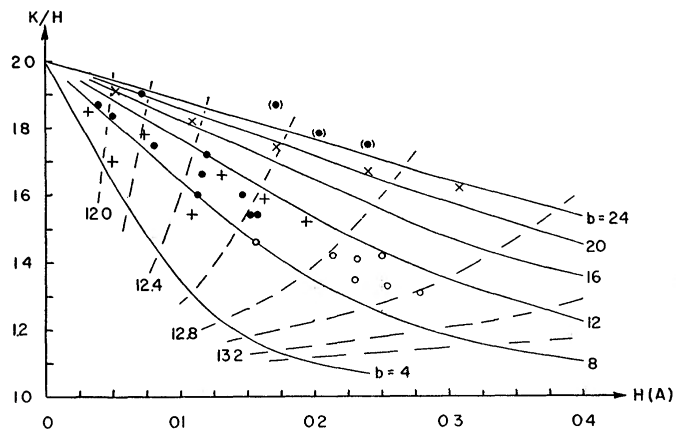

FIG. 9.—Doublet-ratio-curves of the Ca II lines for a Gaussian velocity law of dispersion b. The solid lines represent the loci of constant b and are labeled at their right ends by the value of b in km/sec. The broken lines represent loci of constant number of atoms along the line of sight, N, and are labeled at their left ends by the values of log N. The empty circles represent mean values observed in the Orion arm; the dots refer to observed values in the Perseus arm, the three inclosed in parentheses representing stars in h and χ Persei; the + signs denote mean values as given by Binnendijk, while the $\times$ signs are the mean values adopted by Jentzsch and Unsöld.

Orion arm. In the upper part of Figures 8 and 9, however, there appear three points inclosed in parentheses representing the stars HD 13854, HD 14134, and HD 14143, members of the h and χ Persei cluster. The spectral types of these stars are B1, B2, and B3, respectively, with luminosity class I*a*. Accordingly, the presence of the Ca II stellar lines should be expected to produce somewhat spurious values for the interstellar doublet ratio. The appearance and shape of the V-component of the K line (see Figs. 2 and 4) in these stars is quite unusual for an interstellar line, but they do not look like the stellar K line of other cB stars either, as may be noticed in the lines in HD 14818, a B2 I*a* not too far from the double cluster. The stellar K line in early cB stars has a width between 1 and 2 A, but the central depth is only between 5 and 10 per cent of the continuum (Spitzer *et al.* 1950). It is thus believed that, although the value $\eta = 20$ km/sec indicated by the interstellar Ca II line intensities in stars of the double cluster may be exaggerated by the presence of the stellar lines, there can be hardly any doubt that the interstellar gas in the close neighborhood of the cluster is characterized by an anomalously high turbulent velocity. The nearly normal behavior of the Na I doublet in the same stars may be understood by recalling that in nearby stars it has been observed (Routly and Spitzer

1952) that the ratio N(Na I)/N(Ca II) decreases as the peculiar velocity of the particular cloud increases. Actual proof that the relative concentration of Ca II and Na I changes from place to place near the double cluster is provided by the nearly identical shapes of the V-components of the K line in HD 14134 and HD 14143 and the quite different strength of the same components of Na I in the same stars (see Figs. 1 and 4). A more striking example of variations in the ratio N(Na I)/N(Ca II) in this region is offered by the star HD 14818, where the V1- and V2-components of Ca II are of nearly equal strength, while the V2-component of D2 is much weaker than the V1-component (see Figs. 1, 2, and 4).

VI. CONCLUDING REMARKS

We have shown in the preceding sections that the observed doublet-ratio-curves of Na I and Ca II may be explained by a velocity distribution of a simple exponential type such as equation (3), with a mean speed η independent of position within a spiral arm. For stars in the Orion arm, values for η (Ca II) between 5 and 6 km/sec have been found, while η (Na I) is 1.5 to 1.8 times smaller. In this context it should be recalled that Blaauw (1952) found, from the study of the velocities of multiple lines of Ca II in relatively near-by stars, η (Ca II) = 5 km/sec, with a mean error of 20 per cent, in excellent agreement with our results. For stars in the Perseus arm we have found an indication that η (Na I) may have values between 4 and 5 km/sec, significantly larger than in the Orion arm.

In order to explain the observed doublet-ratio-curves in terms of a Gaussian velocity distribution, on the other hand, a systematic increase of the mean speed with distance from the sun is required. Such a requirement would be difficult not only to explain but even to visualize, considering the probable origin of the mass motions in the interstellar medium. It has been shown by Oort and Spitzer (1955) that the energy dissipated in the interstellar turbulence can be maintained only by radiation energy from high-temperature stars. The transfer of energy between the H II regions and the general medium takes place by means of the high-velocity clouds, which undoubtedly are of small dimensions compared with the thickness of a spiral arm. And a Gaussian law fails to account precisely for the high frequency with which high-velocity components are observed. This observational evidence would seem to be incompatible with a spectrum of turbulence in the interstellar medium such that the velocities increase with eddy sizes up to the largest eddies present, as has been suggested by Unsöld. (The paper in which this idea is advanced by Unsöld is unavailable to the writer, except for the reference found at the end of Section III*d* of a paper by Spitzer [1948].)

The preceding remarks should not be understood in the sense that the exponential distribution of velocities with a constant η applies everywhere. Indeed, attention has been called to the regions close to $l = 85°$ and around h and χ Persei, where we have observed a large excess of high-velocity components. Also from a theoretical standpoint, as we shall comment later, one would expect the mean space density of high-velocity clouds to depend on position. But if for a general purpose it is required to give a single function representing the probability density of the velocities of interstellar clouds, there is no question that the exponential type of equation (3) represents satisfactorily the observed facts. It may be the case that, for a special problem, the concept of velocity distribution is not quite meaningful if it is to describe the kinematics of a medium in which the physical state (pressure, temperature, density) is related to the velocity. In particular, the problem of deciding whether η (Ca II) or η (Na I) should be taken as representative of the interstellar medium in general has to be solved by additional considerations. It is only by the profiles of the 21-cm line of hydrogen (van de Hulst *et al.* 1954) that we know the "effective" η to be nearly equal to η (Ca II).

On the basis of the hypothesis advanced by Oort and Spitzer (1955) to explain the state of motion of interstellar clouds, it is not difficult to understand the existence of variations in the velocity distribution. Since high-velocity clouds are accelerated in the neighborhood of extensive H II regions, it would seem clear that in a volume of space separated from H II regions by a distance larger than the "mean free path" of a high-velocity cloud (of the order of 100 pc), we shall find, on the average, fewer high-velocity clouds than at closer distances. Actually, this situation is observed, for most of the interstellar components with large displacements detected in relatively nearby stars can be related to the presence of O associations (Oort 1954). The space distribution of interstellar hydrogen, as given by van de Hulst *et al.* (1954) in Figure 16 of their paper, also shows the relation of the H II regions to variations in the velocity distribution. The large H II complexes of Orion and Monoceros are found between $l = 165°$ and $l = 175°$. And it is precisely in this region that the Dutch astronomers found in the space distribution of hydrogen, under the assumption of $\eta =$ Constant, striking elongated features pointing toward the sun. As we mentioned before in Section IV*b*, these features undoubtedly result from departures of the actual velocity distribution from the assumed constant one.

In conclusion we shall comment briefly on the role that the high-velocity clouds may play in relation to the phenomenon of spiral structure in general. The "lifetime" of a high-velocity cloud, according to the ideas of Oort and Spitzer (1955), is determined by the collision rate with other clouds and the drag of a possible low-density intercloud medium. It follows that if one such cloud is accelerated in a direction where the over-all mean space density of diffuse matter is low, it would exist as a unit for a longer time than if its motion were directed toward regions of higher density. Thus clouds accelerated in directions pointing away from the center of a spiral arm will move longer distances than those moving toward the center, if they originate in the periphery of the arm. In the direction perpendicular to the galactic plane, the writer (1956) has observed clouds at distances $z > 500$ pc which have existed for 50×10^6 years. Further, there is no force preventing high-velocity clouds from moving into the interarm medium, once they receive the proper acceleration in direction and magnitude. And, independently of the nature of the forces holding the spiral arm together, one would expect, in the interarm medium, high-velocity clouds to be relatively more frequent than in the arms. With this picture in mind, it is tempting to speculate whether a state of pressure quasi-equilibrium might not be reached between the high-velocity clouds in the interarm regions and the slow-moving clouds in the arms. This idea has some similarity to the one advanced recently by Spitzer (1956), who considers that the spiral arms might be in pressure equilibrium (of a hydrostatic rather than turbulent nature) with a high-temperature medium. It would be, of course, of great interest to find observational evidence for the existence of the interarm high-velocity clouds. Our observations of the large number of high-velocity components in stars of the Perseus arm around $l = 85°$ in this connection are suggestive, although far more extensive material would be required to prove that the velocity distribution is actually different in directions perpendicular to and along the spiral arms.

REFERENCES

Adams, W S. 1949, *Ap J*, **109**, 354

Batchelor, G K. 1953, *The Theory of Homogeneous Turbulence* (Cambridge: At the University Press), chap. viii.

Beals, C. S. 1934, M.N, **94**, 663.

———. 1936, *ibid.*, **96**, 661.

Beals, C. S, and Oke, J. B. 1953, *M.N*, **113**, 530.

Binnendijk, L 1952, *Ap. J*, **115**, 428.

Blaauw, A. 1952, *B.A N.*, **11**, 459 (No 436).

Bowen, I S. 1952, *Ap J*, **116**, 1.

Cayrel, R. 1953, *Ann d'ap*, **16**, 129

Deutsch, A. J. 1954, *J. Opt Soc. America*, **44**, 492.

Hulst, H. C. van de, Müller, C. A, and Oort, J. H. 1954, *B. A. N.* **12**, 117 (No 452).

Jentzsch, C., and Unsöld, A. 1948, *Zs. f. Phys.*, **125**, 370.

Kahn, F D 1954, *B.A N.*, **12**, 187 (No. 456).
Lighthill, M J. 1955, *Gas Dynamics of Cosmic Clouds* (Amsterdam: North Holland Publishing Co), chap xxii.
Merrill, P. W , and Sanford, R. F. 1938, *Ap J* , **87**, 118
Merrill, P W., Sanford, R. F , Wilson, O C , and Burwell, C G 1937, *Ap J* , **86**, 205.
Morgan, W W , Code, A. D , and Whitford, A E 1955, *Ap J. Suppl.*, **2**, 41
Morgan, W W , Sharpless, S., and Osterbrock, D. E. 1952, *A J* , **57**, 3.
Morgan, W W., Whitford, A E , and Code, A D. 1953, *Ap J* , **118**, 318.
Münch, G. 1953, *Pub A.S.P.*, **65**, 179
——— 1956, in preparation
Oort, J H. 1954, *B A N* , **12**, 177 (No. 455).
Oort, J. H , and Spitzer, L , Jr. 1955, *Ap. J* , **121**, 6
Routly, P. M., and Spitzer, L., Jr 1952, *Ap. J* , **115**, 227.
Sanford, R. F., and Wilson, O. C. 1939, *Ap. J.*, **90**, 235.
Savedoff, M P , and Greene, J. 1955, *Ap J* , **122**, 477.
Sharpless, S. 1955, *A J* , **60**, 178.
Spitzer, L., Jr 1948, *Ap J.*, **108**, 276.
——— 1956, *Ap. J* , **124**, 20
Spitzer, L , Jr , Epstein, I., and Hen, Li. 1950, *Ann. d'ap.*, **13**, 147.
Strömgren, B. 1948, *Ap. J.*, **108**, 242.
Williams, E. G. 1934, *Ap. J.*, **79**, 280.
Wilson, O C , and Merrill, P. W. 1937, *Ap. J.* **86**, 129.
Wilson, R. E 1953, *General Catalogue of Stellar Radial Velocities* (Washington, D.C.: Carnegie Institution of Washington).